Understanding start-up problems in yeast glycolysis

Overal, Gosse B.; Teusink, Bas; Bruggeman, Frank J.; Hulshof, Josephus; Planqué, Robert

published in
Mathematical Biosciences
2018

DOI (link to publisher)
10.1016/j.mbs.2018.03.007

document version
Publisher's PDF, also known as Version of record

Mathematical Biosciences 299 (2018) 117–126

Contents lists available at ScienceDirect

Mathematical Biosciences

journal homepage: www.elsevier.com/locate/mbs

Understanding start-up problems in yeast glycolysis

Gosse B. Overal[a], Bas Teusink[b], Frank J. Bruggeman[b], Josephus Hulshof[a], Robert Planqué[*,a]

[a] Department of Mathematics, Vrije Universiteit Amsterdam, De Boelelaan 1081, Amsterdam 1081 HV, The Netherlands
[b] Systems Bioinformatics, Faculty of Earth and Life Sciences, Vrije Universiteit Amsterdam, De Boelelaan 1108, Amsterdam 1081 HZ, The Netherlands

ARTICLE INFO

Keywords:
Biochemical pathways
Differential equations
Bifurcation analysis
Glycolysis
Yeast

ABSTRACT

Yeast glycolysis has been the focus of research for decades, yet a number of dynamical aspects of yeast glycolysis remain poorly understood at present. If nutrients are scarce, yeast will provide its catabolic and energetic needs with other pathways, but the enzymes catalysing upper glycolytic fluxes are still expressed. We conjecture that this overexpression facilitates the rapid transition to glycolysis in case of a sudden increase in nutrient concentration. However, if starved yeast is presented with abundant glucose, it can enter into an imbalanced state where glycolytic intermediates keep accumulating, leading to arrested growth and cell death. The bistability between regularly functioning and imbalanced phenotypes has been shown to depend on redox balance.

We shed new light on these phenomena with a mathematical analysis of an ordinary differential equation model, including NADH to account for the redox balance. In order to gain qualitative insight, most of the analysis is parameter-free, i.e., without assigning a numerical value to any of the parameters.

The model has a subtle bifurcation at the switch between an inviable equilibrium state and stable flux through glycolysis. This switch occurs if the ratio between the flux through upper glycolysis and ATP consumption rate of the cell exceeds a fixed threshold. If the enzymes of upper glycolysis would be barely expressed, our model predicts that there will be no glycolytic flux, even if external glucose would be at growth-permissable levels. The existence of the imbalanced state can be found for certain parameter conditions independent of the mentioned bifurcation. The parameter-free analysis proved too complex to directly gain insight into the imbalanced states, but the starting point of a branch of imbalanced states can be shown to exist in detail. Moreover, the analysis offers the key ingredients necessary for successful numerical continuation, which highlight the existence of this bistability and the influence of the redox balance.

1. Introduction

Metabolism is central to all life. The underlying network of enzyme-catalysed reactions adapts to environmental conditions, in order to keep sustaining the living state. In microorganisms metabolism is arguably even more important, since metabolic rates are directly coupled to cellular growth rate, and hence to fitness. Understanding the dynamics of metabolic networks is therefore an important challenge in systems biology.

The glycolysis pathway has been the focus of research for decades. It metabolises glucose into pyruvate, thereby using the free energy to generate 2-adenine5′-triphosphate (ATP) and the freed electrons to reduce nicotinamide adenine dinucleotide (NAD) to NADH. Glycolysis is essential for cells: it provides much of the ATP that drives countless biological processes, and glycolysis provides some of the most important precursor molecules, such as pyruvate, from which amino acids, lipids and other macromolecules are synthesised. Moreover, many metabolic branches feed into glycolysis, so that other sugars, such as fructose, galactose, sucrose, maltose, lactose and others, may be metabolised through this pathway as well.

When yeast is deprived of oxygen, its glycolysis converts pyruvate further into ethanol and CO_2 by oxidising NADH. This yields a very fast but inefficient energy production, in which 2 out of the potential 12 ATP are obtained from one molecule of glucose. The yeast glycolytic pathway has been studied extensively, and two fully detailed models have been developed which include fully parameterised reaction kinetics for all the individual enzymatic steps [9,15]. Nevertheless, despite this wealth of detail, a number of dynamical aspects of yeast glycolysis remain poorly understood at present.

When fermentable nutrients such as glucose or galactose are starting to run out, the expression of glycolytic enzymes is downregulated. The levels of the protein glycolytic regulator 1 (gcr1) drop dramatically [7], inducing this regulation. The flux through glycolysis decreases and the cell enters a state of quiescence. However, gcr1 only binds to the

* Corresponding author.
E-mail address: r.planque@vu.nl (R. Planqué).

https://doi.org/10.1016/j.mbs.2018.03.007
Received 10 February 2017; Received in revised form 19 December 2017; Accepted 7 March 2018
Available online 15 March 2018
0025-5564/

transcription binding sites of lower glycolytic enzymes [2], while upper glycolysis is constitutively expressed, which is often contributed to their double role as glycolytic and gluconeogenic enzymes [2,17].

If some nutrient like glucose would suddenly become readily available, already having a functional upper glycolysis would spark a rise in many catabolic precursors and free energetic ATP. In this paper we will show that this spark immediately allows flux through glycolysis to start, before enzyme levels may be adjusted through regulation. Cells that have the sufficient expression in upper glycolysis will therefore outcompete their neighbours in the metabolic timescale, giving them an evolutionary advantage. Our work also shows that the concentrations of the lower glycolytic enzymes do not influence this threshold, which shows that only the upper glycolytic enzymes need to be expressed when the pathway is inactive to achieve this.

Yeast glycolysis has held another mystery for years. Yeast can synthesise trehalose from the glycolytic intermediate glucose 6-phosphate. This reaction is not a step of the glycolysis pathway, so one does not expect glycolysis to fail when this reaction is disabled by means of a gene knockout. However, many cells of the mutant in which this particular knockout is performed, the tps1-Δ mutant, are not able to grow on glucose [18]. In [18] it was revealed that this mutant shows a form of bistability between a regular steady state and an imbalanced state in which some intermediate metabolites, including fructose-1,6-biphosphate (FBP), accumulate in the cell, reaching toxic levels. In fact, also wild type yeast suffers from this problem, but only a small part of the wild type population enters the imbalanced state [18]. The trehalose branch does not completely inhibit this effect, but makes it less likely for glycolysis to fail and more likely to grow well; in dynamical systems terms: the basin of attraction of the imbalanced state is reduced in size, so that the regular steady state is reached from a wider range of initial conditions. In the analysis of a small core model of yeast glycolysis in the tps1-Δ knockout [13], containing FBP, ATP and inorganic phosphate p_i as dynamic variable, the bistability between regular and imbalanced states was shown to exist, in line with experiments [18].

The tps1-Δ mutant experiments show that the size of the subpopulation entering the imbalanced state is dramatically increased by removing the trehalose branch. By experimentally increasing the ethanol concentration, a distinct influence on the size of the imbalanced subpopulation was shown [18]. The effect of more ethanol, however, could be contributed completely to a heightened NADH/NAD balance, yielding a higher flux through the glycerol producing, and FBP consuming, branch. Lower FBP levels facilitate convergence to a vital steady state with normal glycolytic flux. Theoretically, this influence of redox balance was not taken into account in the previous core model [13]. Here, we shed light on the influence of redox balanced by including NADH and NAD as dynamic variables.

When the metabolite concentrations external to the cell change, for instance if a new food source becomes abundant, the cell's limited enzyme production needs to be redistributed by the gene regulatory network to reach a new steady state to maximise the flux through glycolysis. It has recently been shown that enzyme levels are indeed pervasively tuned to maximise growth rate in yeast [10]. The gene network is responsible for tuning enzyme levels, but it needs input from the pathway it controls to sense changes in the environment. Nutrient-specific membrane receptors could provide such input, and yeast has a detailed glucose-sensing mechanism [5]. Nevertheless, as in most bacteria [11], yeast cells also sense the flux through glycolysis by using glycolytic intermediates binding to transcription factors. These then influence gene expression. Experimental evidence suggests that FBP acts as such a flux sensor [4,8], directly influencing the gene network and thereby inducing changes in the glycolytic enzyme levels, a form of adaptive control [14].

However, it is less clear why FBP should play this role as sensor. For FBP to function properly, its concentration should contain sufficient information to assess the metabolic flux through glycolysis. The FBP concentration should therefore be associated to a unique steady state concentration profile. This has been shown to be true experimentally and a mechanism has been proposed [11], but it is not clear how this property emerges from the kinetic properties of the glycolytic pathway. We investigate here for a detailed core model under what parameter assumptions FBP indeed parametrises steady states. We also ask the question whether the steady states may actually be faithfully predicted by a flux value, for instance one of the FBP-consuming fluxes. Although we will show broadly applicable parameter conditions which yield these phenomena, we do not include dynamic enzyme concentrations or regulation. Therefore our results indicate that the glycolytic pathway generally has kinetic properties that facilitate FBP to function as a flux sensor.

1.1. Introducing the glycolytic pathway

The essential elements of the phenomena described above are the inclusion of FBP (f), ATP (a), inorganic phosphate (p) and NADH (n) as dynamical variables, upper glycolysis (v_1), lower glycolysis (v_2), the glycerol branch (v_3) ethanol production (v_4) and phosphate exchange with the vacuole (v_7) as fluxes. The glycerol pathway is a net consumer of NADH and ethanol is NADH-neutral, so we need to include the succinate pathway (v_5) as a net producer of NADH and cannot lump v_2 and v_4 as v_5 uses the intermediate pyruvate (y) as its input. Then the ethanol pathway is producing ATP and we model all ATP consuming fluxes in the cell in the lumped flux v_6. This model (Fig. 1) is the simplest possible to describe the phenomena of interest, yet already its complexity is high in the context of qualitative analysis of core models.

We consider the metabolic timescale after a sudden increase in external glucose concentration. In this timeframe we assume that the external conditions are constant, such that the growth-permissable glucose and negligable ethanol concentrations are fixed parameters. The concentrations of glycerol and succinate are disregarded with the assumption of product insensitivity of v_3 and v_5, respectively.

The p_i concentration is dynamically buffered (v_7) by diffusion between the cytosol and the vacuole. We assume that the concentration inside the vacuole is not influenced on our timescale and is constant (Π). Therefore, p will be steered towards Π by v_7, the concentration of inorganic phosphate in the vacuole.

Conservation laws dictate the concentrations of ADP and NAD. The total concentration of ATP and ADP is constant (a_T) and so the ADP concentration ($a_T - a$) is a dependent variable. Likewise the NAD concentration ($n_T - n$) is a dependent variable. The parameters a_T and n_T are determined by the initial conditions.

The reactions in the model are lumped, and therefore we cannot use the detailed rate functions given in the Teusink or Hynne models [9,15]. Instead, we have chosen to model them after a few important properties, monotone increasing in the substrate concentration, saturating, irreversible and product insensitive. The underlying assumption

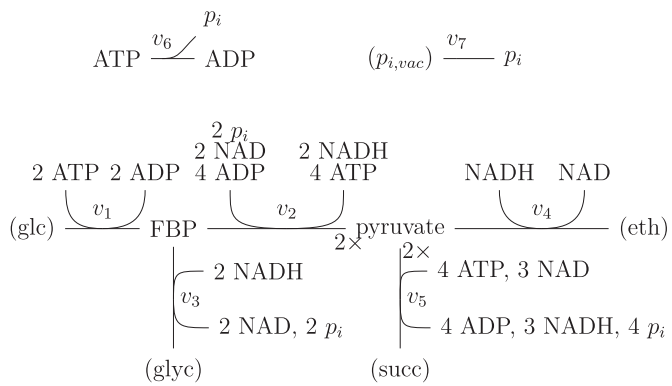

Fig. 1. A graphical representation of the stoichiometry of our model. The nodes are the different metabolites, the arrows are the reactions. When a metabolite species is between brackets, the concentration is disregarded or assumed constant in the model.

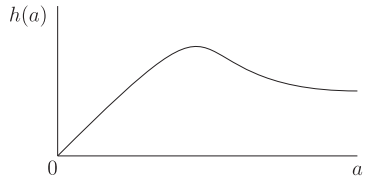

Fig. 2. Schematic illustration of $h(a)$, with $h'(0) = 1$ i.e. $v_1'(0) = V_1$.

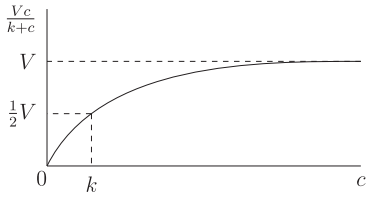

Fig. 3. Michaels-Menten kinetics for substrate concentration c with parameters V and k.

for irreversibility/product insensitivity is the common way to consider PFK, which dominates the rate of upper glycolysis (v_1); we also model the cell as having a major glycolytic flux, making all fluxes very directional. For this reason the fluxes v_2, v_3, v_4 and v_5 are irreversible Michaelis–Menten type dynamics (see Fig. 3). The reaction v_1 in our model corresponds to phosphofructokinase (PFK), a complex enzyme with many binding sites for allosteric activation and inhibition and insensitive for its product FBP, which allows for its indefinite accumulation in the imbalanced state. We simplify here by assuming that v_1 depends only on a [6]. Despite this simplification, PFK still catalyses the most complex reaction: as a function of a, v_1 is not always monotone. The reaction flux increases for small a, because ATP is a substrate, but at some point decreases, because ATP also allosterically inhibits PFK (see Fig. 2 for a sketch). This is a simplification of the reality where the allosteric effect is indirectly effected through AMP [15].

For a more detailed mathematical description, the reader is referred to Section 2.

1.2. A first overview of the main techniques and results

In this section we only introduce the structure of the model, delaying a full description to Section 2, and give a first overview of the main techniques and results.

The independent variables of the model are the concentrations of FBP (f), p_i (p), pyruvate (y), ATP (a) and NADH (n), which are collected in the vector $\boldsymbol{x}$, and 7 reactions $v_1, \ldots, v_7$ collected in $\boldsymbol{v}(\boldsymbol{x})$. The model is a system of differential equations,

$$\dot{\boldsymbol{x}} = N\boldsymbol{v}(\boldsymbol{x}),$$

with stoichiometric matrix N and reaction rates $\boldsymbol{v}(\boldsymbol{x})$ detailed in Section 2. Each row of N denotes how many molecules of that metabolite are used as a substrate (negative entries), or produced (positive entries), by the 7 reactions.

The main goal is to shed light on the change in steady state behaviour of the model, using a natural bifurcation parameter. All three types of behaviour (equilibrium, regular and imbalanced states) have been documented in yeast glycolysis, and will be studied.

To facilitate steady state analysis, we need to separate the variables and fluxes as much as possible. Mathematically, any basis of the row space of N, Row$N$, yields the same null space and therefore the same steady states. In Section 3.1 we will give several bases, each of which is useful for a different part of the analysis. A general method to find such a basis is detailed in the Supplementary information (SI).

For each parameter choice, there will typically be one or several regular steady states that together with their stability describe the behaviour of the model for this choice of parameters. A perturbation of some parameter will perturb also the steady states and/or stability. A standard technique in bifurcation analysis is to consider one parameter as a continuous variable, the bifurcation parameter λ, and follow the steady states along this continuously changing curve. These curves can then have special points of interest with clear meaning, such as two curves intersecting and exchanging stability (a transcritical bifurcation). There is a rich availability of possible parameters, but given the phenomena of interest, the most obvious choice is $\lambda = V_1$. This parameter corresponds to the $V_{\max}$ parameter of v_1. In our model, it incorporates both the abundance of glucose and the enzyme levels of upper glycolysis. Both have been shown to influence whether yeast cells have problems starting up glycolysis, work normally, or indeed keep accumulating glycolytic intermediates.

The equilibrium states, where there is zero flux, are shown to be two axes of the phase space and at the intersection of these there is a (complicated) bifurcation of a simple eigenvalue, a transcritical bifurcation. To show how this bifurcation unfolds, we need an explicit expansion of the emergent curve of steady states. This allows us to show that the regular steady states exist whenever (Theorem 3). This shows that glycolysis will only start up if the upper glycolytic flux crosses a lower bound with respect to the ATP consumption in the cell.

We prove that all non-equilibrium steady states are locally described by a single, one-dimensional curve and that the FBP concentration parameterises this curve under a mild parameter condition (Theorem 4). Although this does not lead to new biological insights, it shows that the model does what it is supposed to do; the setup of the model is to describe a functional cell with glycolysis as the most dominant pathway in its metabolism, but from just the construction it is unclear whether or not the model actually incorporates the normal behaviour of a cell.

The most tangible way of considering the imbalanced state without numerical simulation is to continue the curve of steady states until it reaches an asymptote where FBP approaches infinity. To compactify the state space, we use a coordinate transform from the metabolites to some fluxes to explicitly solve most steady state equations, reducing them to one equation in two flux variables. In the transformed variables, the imbalanced states are finite points instead of asymptotic points. In this way we show that the glycerol flux v_3 parametrises all steady states for some mild parameter conditions. This part of the analysis provides the main justification to set up numerical continuations, but does not provide direct biological insight. It is therefore included in the SI for the interested reader.

The imbalanced states start at the endpoint of the curve of regular steady states. In Section 3.4 we show that V_4 determines precisely where this endpoint lies. We also show that this analysis provides insight into the influence of increased ethanol on the imbalanced behaviour. As an aside, we show that the pyruvate concentration can also reach infinity in our model, which is not comparable to the living cell, but has been an obstacle in previous detailed models of glycolysis [15].

To summarise, given growth-permissable glucose levels, the switch to glycolysis can only be achieved if the cell has a high enough expression of the enzymes in upper glycolysis compared to the ATP consumption of the cell. This emergent curve of regular steady states can be continued until FBP reaches infinity at a finite value of V_1. In Section 3.5, we illustrate the coexistence between regular and imbalanced states numerically. Although this is a simulation for a specific parametrisation, our analysis so far has shown that its characteristics are pervasive for other choices of parameters.

2. The mathematical model

In complete detail, the system of equations is

$$\dot{\boldsymbol{x}} = N\boldsymbol{v}(\boldsymbol{x}),$$

where $\boldsymbol{x}$, N, and $\boldsymbol{v}$ are

$$\boldsymbol{x} = \begin{pmatrix} f \\ p \\ y \\ a \\ n \end{pmatrix}, \qquad N = \begin{array}{c} \\ f \\ p \\ y \\ a \\ n \end{array} \begin{array}{c} \begin{array}{ccccccc} v_1 & v_2 & v_3 & v_4 & v_5 & v_6 & v_7 \end{array} \\ \begin{pmatrix} 1 & -1 & -1 & 0 & 0 & 0 & 0 \\ 0 & -2 & 2 & 0 & 4 & 1 & 1 \\ 0 & 2 & 0 & -1 & -2 & 0 & 0 \\ -2 & 4 & 0 & 0 & -4 & -1 & 0 \\ 0 & 2 & -2 & -1 & 3 & 0 & 0 \end{pmatrix} \end{array}, \tag{1}$$

$$\boldsymbol{v} = \begin{pmatrix} v_1 \\ v_2 \\ v_3 \\ v_4 \\ v_5 \\ v_6 \\ v_7 \end{pmatrix} = \begin{pmatrix} V_1 h(a) \\ V_2 \dfrac{f}{k_{2,f}+f} \dfrac{p}{k_{2,p}+p} \dfrac{a_T - a}{k_{2,a}+a_T-a} \dfrac{n_T - n}{k_{2,n}+n_T-n} \\ V_3 \dfrac{f}{k_{3,f}+f} \dfrac{n}{k_{3,n}+n} \\ V_4 \dfrac{y}{k_{4,y}+y} \dfrac{n}{k_{4,n}+n} \\ V_5 \dfrac{y}{k_{5,y}+y} \dfrac{a}{k_{5,a}+a} \dfrac{n_T - n}{k_{5,n}+n_T-n} \\ V_6 a \\ V_7(\Pi - p) \end{pmatrix}. \tag{2}$$

For the variables in $\boldsymbol{x}$, we demand

$$f, y, p \in \mathbb{R}_{\geq 0},\ a \in [0, a_T],\ n \in [0, n_T]. \tag{3}$$

In the definitions of the reaction rates, all parameters are positive and $h(a)$ is defined as follows (see also Fig. 2 for a sketch),

$$h(a) = \frac{a(d_1 + a)(d_1^2 + L(K + d_3)^2)}{d_1(d_1 + a)^2 + d_1 L\left(\frac{K + d_2 a}{K + a}\right)^2 (K + d_3)^2}. \tag{4}$$

The parameters d_1, d_2, d_3, and d_4 are also positive. This formula is based on [15], where the concentrations of all metabolites apart from a are assumed to be constant [6], and V_1 is rescaled such that $h'(0) = 1$.

The bifurcation parameter is $\lambda = V_1 \geq 0$.

3. Steady state analysis

The goal of this section is to gain insight into the steady states; steady states are solutions $\boldsymbol{x}$ to the steady state equations, given by

$$N\boldsymbol{v}(\boldsymbol{x}) = \boldsymbol{0}, \tag{5}$$

with $\boldsymbol{x}$, N, and $\boldsymbol{v}$ defined as in (1) and (2). We aim to solve these equations for $\boldsymbol{x}$ and the bifurcation parameter $\lambda = V_1$.

3.1. Suitable representations of the null space of N

We provide a general method to construct different bases of Row$N$ in the SI, which separate fluxes and variables as much as possible. The new version of the steady state equations that are used throughout the paper are given by

$$\widetilde{N}_{36} := \begin{pmatrix} 10 & 0 & -28 & 0 & 0 & -5 & 0 \\ 0 & 10 & -18 & 0 & 0 & -5 & 0 \\ 0 & 0 & -14 & 5 & 0 & -5 & 0 \\ 0 & 0 & -2 & 0 & 5 & 0 & 0 \\ 0 & 0 & 0 & 0 & 0 & 0 & 1 \end{pmatrix}. \tag{6}$$

In the SI we also use two other versions of this matrix, denoted $\widetilde{N}_{56}$ and $\widetilde{N}_{356}$. Each is useful for a certain part of the analysis.

3.2. The equilibrium states

The system has trivial solutions, which we refer to in this work as equilibrium states.

Definition 1. A state $\boldsymbol{x}$ is called an equilibrium state if $\boldsymbol{v}(\boldsymbol{x}) = \boldsymbol{0}$.

Chemical equilibria are usually dynamical steady states, where the forward and backward reactions are balanced, but in our model nearly all reactions are irreversible (the exception being v_7). As a modelling artefact, the equilibrium states in our model are not balanced in forward and backward reactions, but have zero forward and zero backward reaction rates. They therefore cannot represent a living cell. Nevertheless, the V_1 parameter, which includes both glucose availability and upper glycolytic enzyme concentrations, is an important parameter. Starved yeast cells do sometimes have problems starting up glycolysis, even when offered abundant glucose. We are therefore interested if and how the glycolytic pathway behaves for lower values of V_1.

Lemma 2. *The equilibrium states are* $\boldsymbol{x} = \begin{pmatrix} f \\ p \\ y \\ a \\ n \end{pmatrix} = \begin{pmatrix} 0 \\ \Pi \\ y \\ 0 \\ n \end{pmatrix}$, *where* $yn = 0$.

The proof can be found in the SI. The equilibrium states are a family of two lines on the boundary of the metabolite space. Either $(0, \Pi, 0, 0, n)$, where $n \in [0, n_T]$ or $(0, \Pi, y, 0, 0)$, where $y \in \mathbb{R}_{\geq 0}$. The intersection of these two families is the equilibrium

$$\boldsymbol{x}_0 = \begin{pmatrix} 0 \\ \Pi \\ 0 \\ 0 \\ 0 \end{pmatrix}.$$

In the SI we show that $\boldsymbol{x}_0$ is, in fact, the only relevant equilibrium, because a transcritical bifurcation occurs at $\boldsymbol{x}_0$, giving rise to the non-equilibrium, or regular, steady states. We also show that any regular steady state that is near the equilibrium states is on this emergent curve. Furthermore, at this bifurcation $\boldsymbol{x}_0$ transfers local stability to the regular non-equilibrium steady states.

The equilibrium state $\boldsymbol{x}_0$ is thus a highly degenerate point, where three families of steady states meet. The bifurcation analysis for this point is therefore quite subtle. The bifurcation point has a quadruple zero, of which three zeros have to be separated before the actual bifurcation becomes emerges.

The curve can even be made explicit as a power series expansion in $t = \lambda - \frac{V_6}{2}$, approximating f, y, a and n around $\left(\boldsymbol{x}_0, \frac{V_6}{2}\right)$ (see SI for details). The variables may be expanded as

$$\begin{aligned} f &= f_2 t^2 + f_3 t^3 + \mathcal{O}(t^4), \\ y &= y_1 t + y_2 t^2 + \mathcal{O}(t^3), \\ a &= a_2 t^2 + a_3 t^3 + \mathcal{O}(t^4), \\ n &= n_1 t + n_2 t^2 + \mathcal{O}(t^3), \end{aligned} \tag{7}$$

with all coefficients strictly positive. Therefore the curve enters the domain of biologically relevant ($\boldsymbol{x}$, λ)-space at $V_6/2$, for increasing λ,

because the lowest order terms of the variables are all positive.

Theorem 3. *For any possible choice of parameters, there exists a transcritical bifurcation at $\lambda = V_6/2$, at which the equilibrium state $\boldsymbol{x}_0$ confers stability to the regular steady state.*

We note that, compared to the previously studied core model [13], which lacked NADH and pyruvate, the bifurcation structure is simpler, with an unconditional transcritical bifurcation at $\lambda = V_6/2$.

3.3. Parameterising steady states by metabolite concentrations

In order to investigate whether f may act as a flux sensor at fixed enzyme levels (fixed V_i's), we will show that the bifurcation curve is locally one-dimensional regardless of parametrisation, and, under mild and biologically plausible parameter conditions, can be parametrised by f.

For the following analysis, we will use the matrix $\widetilde{N}_{36}$ (6), since its Jacobian has most entries with a clear sign, irrespective of parameter values. The steady state equations are given by $\widetilde{N}_{36}\boldsymbol{v}(\boldsymbol{x}) = 0$, which can be written out as

$$\begin{pmatrix} 10\lambda h(a) & -28v_3 & -5v_6 \\ 10v_2 & -18v_3 & -5v_6 \\ 5v_4 & -14v_3 & -5v_6 \\ 5v_5 & -2v_3 & \\ V_7(\Pi - p) & & \end{pmatrix} = 0, \tag{8}$$

with $v_2, \ldots, v_6$ as defined in Eq. (2). We now focus on regular steady states in which $f, p, y, a, n > 0$ and $a < a_T$, $n < n_T$. The equations

$$\begin{aligned} 10\lambda h(a) &= 28v_3 + 5v_6, \\ V_7(\Pi - p) &= 0, \end{aligned}$$

are solved by

$$\lambda = \frac{28v_3(f, n) + 5v_6(a)}{10h(a)}, \quad p = \Pi. \tag{9}$$

The solution for p shows that the pathway neither produces nor consumes phosphate in regular steady states. The remaining steady state equations (8) are $K(f, y, a, n) = 0$, where

$$K(f, y, a, n) = \begin{pmatrix} 10v_2(f, \Pi, a, n) & -18v_3(f, n) & -5v_6(a) \\ 5v_4(y, n) & -14v_3(f, n) & -5v_6(a) \\ 5v_5(y, a, n) & -2v_3(f, n) & \end{pmatrix}. \tag{10}$$

Let dK denote the Jacobian matrix of K. Note that we can factor it as follows,

$$\begin{aligned} dK &= \begin{pmatrix} 10\frac{\partial v_2}{\partial f} - 18\frac{\partial v_3}{\partial f} & 0 & 10\frac{\partial v_2}{\partial a} - 5V_6 & 10\frac{\partial v_2}{\partial n} - 18\frac{\partial v_3}{\partial n} \\ 0 & 5\frac{\partial v_4}{\partial y} & -5V_6 & 5\frac{\partial v_4}{\partial n} - 14\frac{\partial v_3}{\partial n} \\ -2\frac{\partial v_3}{\partial f} & 5\frac{\partial v_5}{\partial y} & 5\frac{\partial v_5}{\partial a} & 5\frac{\partial v_5}{\partial n} - 2\frac{\partial v_3}{\partial n} \end{pmatrix} \\ &= \begin{pmatrix} 10 & -18 & 0 & 0 & -5 \\ 0 & -14 & 5 & 0 & -5 \\ 0 & -2 & 0 & 5 & 0 \end{pmatrix} \cdot \begin{pmatrix} \frac{\partial(v_2, v_3, v_4, v_5, v_6)}{\partial(f, y, a, n)} \end{pmatrix} \end{aligned} \tag{11}$$

The left matrix is a submatrix of $\widetilde{N}_{36}$ (6) and we will expand upon the right matrix to reformulate it (12).

With the exception of v_1, the rate functions which make up $\boldsymbol{v}$ are products of individual functions of one variable, in which each function is monotone increasing in its variable (here we include the dependent variables $b = a_T - a$ and $d = n_T - n$ for ADP and NAD respectively). Thus any partial derivative of a reaction to a metabolite yields the same product, where the function of the specific metabolite is replaced with its derivative (with a possible minus in front). Moreover, this structure is independent of the specific values of parameters or variables.

We introduce some notation to capture these properties: let $z_i := \frac{z}{k_{i,z} + z}$. where z is a metabolite concentration and i follows from which flux v_i we consider. For instance, for flux v_3 we get $v_3 = V_3 f_3 n_3$, where $f_3 = \frac{f}{k_{3,f} + f}$ and $n_3 = \frac{n}{k_{3,n} + n}$. In this notation, $\frac{\partial v_3}{\partial f} = V_3 f_3' n_3$, for instance. The possible minus comes from taking a partial derivative to a for a function b_i or likewise for n and d_i, which yields $-b_i'$ or $-d_i'$ respectively. Then multiplying with $1 = \frac{z_i}{z_i}$ we get that the partial derivative to z of a flux is this flux times a logarithmic derivative of its z-dependent function,

$$\frac{\partial v_i}{\partial z} = \pm v_i \frac{z_i'}{z_i}.$$

We use here that z_i is nonzero for any concentration z and flux v_i, which follows from our positivity assumptions on the metabolite concentrations. In this notation, we can rewrite the flux definitions (2) as

$$\begin{pmatrix} v_2 \\ v_3 \\ v_4 \\ v_5 \\ v_6 \end{pmatrix} = \begin{pmatrix} V_2 f_2 p_2 b_2 d_2 \\ V_3 f_3 n_3 \\ V_4 y_4 n_4 \\ V_5 y_5 a_5 d_5 \\ V_6 a \end{pmatrix}.$$

We take partial derivatives to f, y, a and n and rewrite to get

$$\left(\frac{\partial(v_2, v_3, v_4, v_5, v_6)}{\partial(f, y, a, n)}\right) = \begin{pmatrix} v_2\frac{f_2'}{f_2} & 0 & -v_2\frac{b_2'}{b_2} & -v_2\frac{d_2'}{d_2} \\ v_3\frac{f_3'}{f_3} & 0 & 0 & v_3\frac{n_3'}{n_3} \\ 0 & v_4\frac{y_4'}{y_4} & 0 & v_4\frac{n_4'}{n_4} \\ 0 & v_5\frac{y_5'}{y_5} & v_5\frac{a_5'}{a_5} & -v_5\frac{d_5'}{d_5} \\ 0 & 0 & V_6 & 0 \end{pmatrix}. \tag{12}$$

Each of these logarithmic derivatives is positive and the fluxes are also positive. Now we have dK in a form amenable to analysis.

The Jacobian dK has one column more than it has rows; removing a column and computing the determinant yields a subdeterminant. If a subdeterminant is nonzero for a given solution of $K(f, y, a, n) = 0$, then the Implicit Function Theorem (IFT) gives us that the solutions can be locally parameterised in the variable corresponding to the removed column [12]. For example, proving that the subdeterminant where the first column of dK is removed is nonzero for a solution (f, y, a, n), implies that locally the steady states are on a one-dimensional manifold that can be parameterised by the concentration f. We will prove that this is the case.

Theorem 4. *The non-equilibrium steady states can be described as a one-dimensional manifold parameterised by concentration f if*

$$k_{4,n} \geq k_{3,n}. \tag{13}$$

Proof. We only need to show that for any solution of Eq. (10), the subdeterminant of dK, where the first column is removed, is nonzero. We can start at an arbitrary solution and follow the locally defined manifold for decreasing f. We can continue this until the subdeterminant is zero, but the subdeterminant is nonzero for any non-equilibrium steady state and f is decreasing, so we must encounter an equilibrium state, where indeed the subdeterminant is zero. In Section 3.2, we showed that there is only one emergent curve of non-equilibrium steady states from the equilibrium states, hence all steady states are on the same curve, starting at $\boldsymbol{x}_0$ for $f = 0$.

So it remains to be shown that the subdeterminant of dK, where the first column is removed is nonzero for any solution of Eq. (10). Using the reformulation of the Jacobian (12), we can write the relevant subdeterminant as

$$\begin{vmatrix} 0 & -10v_2\frac{b_2'}{b_2} - 5V_6 & -10v_2\frac{d_2'}{d_2} - 18v_3\frac{n_3'}{n_3} \\ 5v_4\frac{y_4'}{y_4} & -5V_6 & 5v_4\frac{n_4'}{n_4} - 14v_3\frac{n_3'}{n_3} \\ 5v_5\frac{y_5'}{y_5} & 5v_5\frac{a_5'}{a_5} & -5v_5\frac{d_5'}{d_5} - 2v_3\frac{n_3'}{n_3} \end{vmatrix}.$$

Writing this out, we can see that it is a sum of three negative terms and

$$-\left(10v_2\frac{b_2'}{b_2} + 5V_6\right)\left(5v_5\frac{y_5'}{y_5}\right)\left(5v_4\frac{n_4'}{n_4} - 14v_3\frac{n_3'}{n_3}\right),$$

where the right factor does not have a clear sign. We see that the entire determinant is negative if this factor is nonnegative,

$$5v_4\frac{n_4'}{n_4} - 14v_3\frac{n_3'}{n_3} \geq 0.$$

To show the above inequality, we use the steady state equations (8). In particular

$$5v_4 = 14v_3 + 5v_6.$$

Substituting this equation for $5v_4$, we see that the subdeterminant is smaller than zero if the following inequality (or its rewritten form below) holds,

$$(14v_3 + 5v_6)\frac{n_4'}{n_4} - 14v_3\frac{n_3'}{n_3} \geq 0,$$
$$14v_3\left(\frac{n_4'}{n_4} - \frac{n_3'}{n_3}\right) + 5v_6\frac{n_4'}{n_4} \geq 0.$$

This would follow from the inequality

$$\frac{n_4'}{n_4} - \frac{n_3'}{n_3} \geq 0,$$

which is a consequence of our assumption $k_{4,n} \geq k_{3,n}$ as we can write out the definitions (2),

$$\frac{n_4'}{n_4} - \frac{n_3'}{n_3} = \frac{k_{4,n}}{(k_{4,n}+n)^2}\frac{k_{4,n}+n}{n} - \frac{k_{3,n}}{(k_{3,n}+n)^2}\frac{k_{3,n}+n}{n}$$
$$= \frac{k_{4,n}(k_{3,n}+n) - k_{3,n}(k_{4,n}+n)}{(k_{3,n}+n)(k_{4,n}+n)n} = \frac{k_{4,n}-k_{3,n}}{(k_{3,n}+n)(k_{4,n}+n)} \geq 0.$$

□

Although the parameter condition of Theorem 4 is comprehensive and acceptable, we can make a more general statement. We now prove that any admissible nonzero vector (f, y, a, n) yields a Jacobian dK where any two subdeterminants are *never both* zero. In this way we prove that any solution lies on a one-dimensional curve of solutions.

Lemma 5. *Given f, p, y, a, $n > 0$ and $a < a_T$, $n < n_T$, then if a 3×3 subdeterminant of dK is 0, then the other subdeterminants are nonzero.*

Proof. Assume, for the sake of contradiction, that two arbitrarily chosen subdeterminants are zero. This yields two equations that must hold. We can rewrite these equations as expressions for V_2 and V_6, because in those parameters, the equations are polynomial. Although this is a cumbersome task, it is elementary. The full computations can be found in the supplementary Mathematica script. The script uses the rewritten form of dK from Eq. (12). The resulting expressions show that $V_2 < 0$ or $V_6 < 0$ follows from the positivity constraints on the other paramters and variables, regardless of their specific values. The parameters V_2 and V_6 are constrained to be positive themselves, so this is a contradiction. We conclude that if one subdeterminant is zero for an admissible solution $\boldsymbol{x}$, the other subdeterminants are nonzero. □

An immediate consequence the Lemma 5 is the following Theorem.

Theorem 6. *All steady state solutions in the interior of the extended metabolite space, $(\boldsymbol{x}, \lambda) > 0$, lie locally on a smooth one-dimensional manifold.*

The curve of steady states can not only be parametrised by f, but also by the flux v_3.

Theorem 7. *All solutions to (5) in $(\boldsymbol{x}, \lambda)$ are on a manifold described as a function of v_3, if the following condition on the parameters is satisfied,*

$$k_{3,f} - k_{2,f} + 2V_2k_{3,f}\frac{\Pi}{k_{2,p}+\Pi}\frac{n_T}{k_{2,n}+n_T}\frac{k_{2,a}}{V_6(k_{2,a}+a_T)^2} > 0. \tag{14}$$

The proof is a long exercise in algebraic manipulation of equations. The reader is referred to the SI, because these details do not contribute to biological insights. To prove this Theorem, the state space is compactified, making the imbalanced states in which $f \to \infty$ finite objects.

3.4. The imbalanced state

We now turn our attention to the imbalanced state in our model. We have seen in Section 3.2 that the regular steady states connect with the equilibrium states at the transcritical bifurcation; the other end of the curve must cross the boundary where f or y is infinite. In this section we show that in fact any such point can be at the end of the regular steady state curve if V_4 is chosen appropriately.

We want to continue the curve of steady states until f approaches infinity. Through a simple coordinate transform this becomes a finite point. This point does not itself signify an imbalanced state, because it is on the nullcline $\dot{f} = 0$. The way to find imbalanced states is to consider all other nullclines and disregard the nullcline for f. This gives a new curve of imbalanced states. If some are stable and coexisting with regular steady states we have shown bistability.

The infinite endpoint of the steady state curve is found and classified below; its continuation was unfortunately beyond our reach with parameter-free analysis. Instead we turn to numerics to confirm the possible bistability and consider the remaining biological questions (Section 3.5).

We will show that in this model, f and y may both keep increasing to infinity, even simultaneously, depending on the parameter V_4. This extends the analysis on the smaller core model discussed in [13], in which this type of bistability was also studied.

First we introduce a coordinate transform to rescale the points "at infinity" to 1. Set

$$\phi = \frac{f}{k_{3,f}+f}, \qquad \rho = \frac{y}{k_{4,y}+y}, \tag{15}$$

so that

$$\psi(\phi) = \frac{f}{k_{2,f}+f} = \frac{\kappa_f\phi}{1+\phi(\kappa_f-1)}, \qquad \kappa_f = \frac{k_{3,f}}{k_{2,f}}, \tag{16}$$

$$\rho_5(\rho) = \frac{y}{k_{5,y}+y} = \frac{\kappa_y\rho}{1+\rho(\kappa_y-1)}, \qquad \kappa_y = \frac{k_{4,y}}{k_{5,y}}, \tag{17}$$

where $\psi(\phi)$ and $\rho_5(\rho)$ map [0, 1] onto [0, 1], and are monotone increasing, one-to-one functions. Note that these functions were also used to prove Theorem 7 and can be found in the SI.

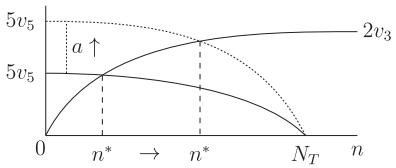

Fig. 4. Schematic representation of (20) in terms of n. As a increases (the dotted graph), n^* is increases.

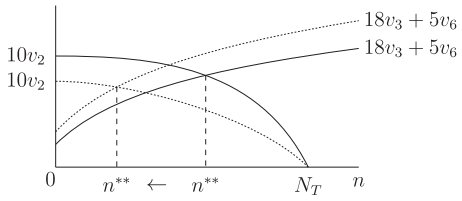

Fig. 5. Schematic representation of (21). The dotted graphs are for larger a, giving smaller n^{**}. Note that $a < a^{**}$ in both cases.

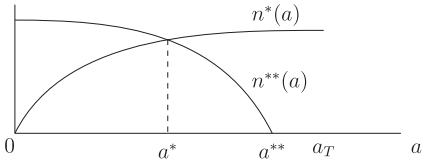

Fig. 6. Eqs. (20) and (21) have a unique solution (a^*, n^*) as the two solutions for n can be solved at the same time with $a = a^*$.

Theorem 8. *For any* $(\phi, \rho) \in (0, 1]^2$, *the point* $(\phi, \Pi, \rho, a^*, n^*, \lambda^*)$ *is a steady state, for a unique* $n^* \in (0, n_T)$, $a^* \in (0, a_T)$ *and* $\lambda^* > 0$, *and a unique value of the parameter* V_4, *given by*

$$V_4 = \frac{7V_5\rho_5 \frac{a^*}{k_{5,a}+a^*}\frac{n_T-n^*}{k_{5,n}+n_T-n^*} + V_6 a^*}{\rho \frac{n^*}{k_{4,n}+n^*}}. \tag{18}$$

Proof. This proof is most easily followed from the schematic graphs in Figs. 4–6.

To prove the lemma, we need all equations to have clear monotonicity properties in the variables a and n. So depending on what this behaviour in the positive part in an equation is, we either choose v_3 or v_5 together with v_6 to complete that equation. For instance, v_2 is monotone decreasing in n, thus in each equation we need the negative parts to be monotone increasing in n; since v_5 is monotone decreasing in n and v_3 is monotone increasing in n, v_3 is the right choice the argument. This leads us to use the following matrix, where only the third row is different than in the matrix $\widetilde{N}_{36}$ used in the previous sections,

$$\begin{pmatrix} 10 & 0 & -28 & 0 & 0 & -5 & 0 \\ 0 & 10 & -18 & 0 & 0 & -5 & 0 \\ 0 & 0 & 0 & 1 & -7 & -1 & 0 \\ 0 & 0 & -2 & 0 & 5 & 0 & 0 \\ 0 & 0 & 0 & 0 & 0 & 0 & 1 \end{pmatrix}. \tag{19}$$

The steady state equations can then be rewritten as

$$2v_3 = 5v_5, \tag{20}$$

$$10v_2 = 18v_3 + 5v_6, \tag{21}$$

$$v_4 = 7v_5 + v_6, \tag{22}$$

together with

$$\lambda = \frac{28v_3 + 5v_6}{10h(a)} \text{ and } p = \Pi.$$

Recall the flux functions (2); written out, the first Eq. (20) is

$$2V_3\phi\frac{n}{k_{3,n}+n} = 5V_5\rho_5\frac{a}{k_{5,a}+a}\frac{n_T-n}{k_{5,n}+n_T-n}.$$

There is a unique solution $n = n^*(a)$: this follows from the IFT, because the lhs is 0 at $n = 0$ and increasing in n, the rhs is 0 at $n = n_T$ and decreasing in n. The function $\hat{n}(a)$ is strictly increasing in a, because $\frac{\partial v_3}{\partial a} = 0$ and $\frac{\partial v_5}{\partial a} > 0$ (see Fig. 4).

The next Eq. (21) written out is

$$10V_2\psi\Pi\frac{a_T-a}{k_{2,a}+a_T-a}\frac{n_T-n}{k_{2,n}+n_T-n} = 18V_3\phi\frac{n}{k_{3,n}+n} + 5V_6 a.$$

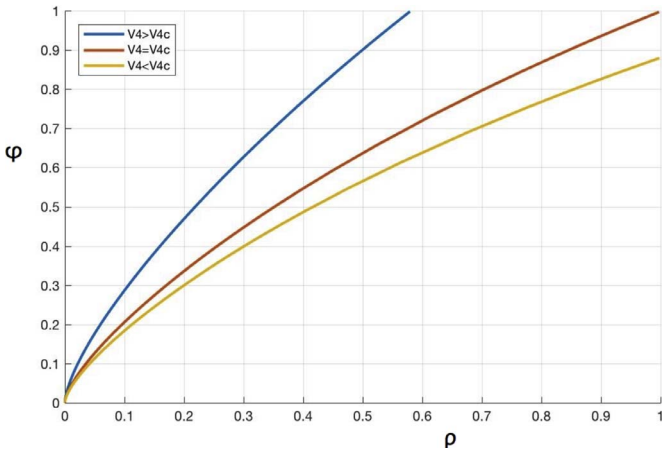

Fig. 7. Numerical illustration of the interpretation of Theorem 8. The steady state curve for three different values of V_4. Note that the curve tends to $f \to \infty$ $(\phi \to 1)$ for smaller values of V_4 and to $y \to \infty$ $(\rho \to 1)$ for larger values. At a critical value $V_4 = V_{4c}$, both tend to infinity simultaneously.

Considered independently from (20), we have a unique solution $n = n^{**}(a)$ if a is small enough: note that the lhs is monotone decreasing and the rhs monotone increasing in n. At $n = n_T$ the lhs is zero and the rhs positive, so we can only use the IFT if, at $n = 0$, there is the inequality

$$10V_2\psi\Pi\frac{a_T-a}{k_{2,a}+a_T-a}\frac{n_T}{k_{2,n}+n_T} > 5V_6 a.$$

For $a = 0$, this inequality holds and by continuity, it will still hold as a increases, with a maximum a^{**}, where the inequality becomes an equality, yielding $n^{**}(a^{**}) = 0$. Therefore $a \in [0, a^{**})$, yields that $n^{**}(a) \in (0, n_T)$ is a solution, which is strictly decreasing in a, because $\frac{\partial v_2}{\partial n} > 0$, $\frac{\partial}{\partial n}(18v_3 + 5v_6) < 0$ (see Fig. 5).

Eqs. (20) and (21) are not independent, so we need that $n^*(a) = n^{**}(a)$. These two solutions of n are the same for a unique $a = a^*$: the solution to (20) $n^*(a)$ is 0 at $a = 0$ and increasing, and the solution to (21) $n^{**}(a)$ is 0 at $a = a^{**}$ and decreasing (see also Fig. 6).

For simplicity, we will denote $n^*(a^*)$ as n^*. Note that n^* and a^* do not depend on V_4.

The last steady state Eq. (22) written out with $n = n^*$ and $a = a^*$ is solved by $V_4 \in \mathbb{R}_+$:

$$V_4 = \frac{7V_5\rho_5 \frac{a^*}{k_{5,a}+a^*}\frac{n_T-n^*}{k_{5,n}+n_T-n^*} + V_6 a^*}{\rho \frac{n^*}{k_{4,n}+n^*}}.$$

If V_4 is this value, the steady state curve will pass through our given $(\phi, \rho) \in (0, 1]^2$ with $a = a^*$ and $n = n^*$ as the remaining variables, and $\lambda = \frac{28v_3(\phi, n^*) + 5v_6(a^*)}{10h(a^*)}$, $p = \Pi$. □

The result of the above lemma implies that the steady state curve can end in any point where $\phi = 1$ or $\rho = 1$ depending on the parameter V_4. This is numerically illustrated by Fig. 7.

Note that within this model, it is possible for pyruvate to accumulate. This is an artifact of this model, and not seen in experiments. However, even in more detailed models like the Teusink model [15] with reversible rate laws and fitted parameters, this phenotype was numerically seen had to be avoided by increasing fermentation, which coincides with increasing our parameter V_4.

The imbalanced state is characterised as having an accumulation of f while the other variables are in steady state. In our analysis, this means that we investigate a steady state of the related model where $\phi = 1$ is fixed and $\dot{f} = 0$ is *not* part of the steady state equations:

$$\dot{\tilde{\boldsymbol{x}}} = \widetilde{N}\boldsymbol{v}(\tilde{\boldsymbol{x}}), \tag{23}$$

where $\phi = 1$, $\tilde{\boldsymbol{x}} = (p, y, a, n)$ and

$$\widetilde{N} = \begin{pmatrix} 0 & -2 & 2 & 0 & 4 & 1 & 1 \\ 0 & 2 & 0 & -1 & -2 & 0 & 0 \\ -2 & 4 & 0 & 0 & 4 & 1 & 0 \\ 0 & 2 & -2 & -1 & 3 & 0 & 0 \end{pmatrix}.$$

We should however have $\dot{f} > 0$ as we want accumulation of f.

If we consider the steady states of this problem without assuming $\phi = 1$, the steady state curve as parameterised by v_3 in Theorem 7 solves these equations, because we have the same equations, without $\dot{\phi} = 0$. Moreover the solutions were nondegenerate (which follows from Lemma 5), so locally the solutions to $\widetilde{N}\boldsymbol{v}(\boldsymbol{x}) = \boldsymbol{0}$ are a curved plane and the steady state curve separates the part where $\dot{f} < 0$ and $\dot{f} > 0$. If the steady state curve connects to a point where $\phi = 1$, this is the starting point of a curve of imbalanced states. We can continue in two directions; one will have $\dot{f} > 0$ and this is the branch we want to follow.

To find out which branch it is, we manipulate $\widetilde{N}\boldsymbol{v} = \boldsymbol{0}$. We sum the first and third rows to see that $\dot{p} + \dot{a} = 0$, which yields

$$\begin{aligned} 0 &= -2v_2 + 2v_3 + 4v_5 + v_6 + v_7 - 2v_1 + 4v_2 - 4v_5 - v_6 \\ &= -2(v_1 - v_2 - v_3) + v_7, \end{aligned}$$

in which we recognise $\dot{f} = v_1 - v_2 - v_3$. We substitute $v_7 = V_7(\Pi - p)$ from (2) to get

$$\dot{f} = \frac{1}{2}V_7(\Pi - p). \tag{24}$$

Hence on the curved plane of solutions to $\widetilde{N}\boldsymbol{v}(\boldsymbol{x})$, we have that $p < \Pi$ is equivalent to $\dot{f} > 0$, thus we follow the branch for decreasing p. This is to be expected biologically: to continue production of FBP, phosphate needs to be added from the vacuole, causing a drop in the vacuole concentration [18].

3.5. Numerical illustrations

In [18] it was shown through experiments and modelling that lower values of upper glycolytic parameters would make it less likely for glycolysis to end up in an imbalanced state. In our model, this would correspond to lower V_1 making it less likely to have a bistable imbalanced state. Second, a higher ethanol concentration, reducing fermentation, was linked to a lower likelihood of an imbalance between upper and lower glycolysis [18]. This higher ethanol pushed the fermentative flux backwards upstream, and caused steady state values of NADH and higher flux through the glycerol branch. In our model ethanol is not included, but we can decrease fermentation by lowering V_4.

Parameter-free analysis of how the regular steady states reach the imbalanced ones (Section 3.4) provides us with the mathematical insight to support parameter manipulations in numerical investigations. We aim to confirm in our model the bistability of steady and imbalanced states and confirm in our model the “rescue mechanisms” of decreased V_4 and decreased V_1.

The bistability is indeed shown to exist (see Fig. 8); the only parameter condition seems to be that V_7 needs to be low enough. This is consistent with previous work [16,18]. The imbalance between upper and lower glycolysis causes a depletion of phosphate by continued production of FBP. This was the reason to include p as a dynamic variable. Limiting the supply of free p by lowering V_7, should therefore make the imbalanced state exist for even lower values of V_1.

What can also be seen in Fig. 8 is that for $\lambda = V_1$ low enough, there is no bistability. So decreased V_1 makes it less likely to have bistability confirming the rescue mechanism of low V_1. The Figure suggests that the curve ends, after which there is no bistability. However, in the numerics we see an accumulation of pyruvate near the end of the curve; for higher V_1 there will be likely be a new imbalanced state with both infinite FBP and pyruvate.

To shed light on the influence of V_4, we tried several values of V_4 and observed the change in the imbalanced states, in particular the NADH and $\lambda = V_1$ values. In Fig. 9 we see the curve of imbalanced states for three different V_4. Lowering the fermentative flux we go from black (highest), through red, to magenta (lowest). There are three patterns of interest that can be seen from this. The entire graph shifts up and to the right. In particular the point where V_1 is minimal also shifts to the right. The point where pyruvate starts accumulating is encountered sooner. The shifting up of the entire graph means a higher NADH, and shifting to the right requires a higher V_1, both of which support the narrative of the rescue mechanism for increased ethanol (lower V_4).

4. Discussion

With the goal of shedding light on aspects of glycolysis (bistability with an imbalanced state, expression of upper glycolytic enzymes when glycolysis is downregulated and FBP functioning as a flux sensor) we have provided an exhaustive mathematical analysis of a core model. The precise mathematical statements are given by Theorems 3, 4, 6 and 7 in Section 3. Their biological interpretation is described below.

4.1. Without overexpression of its upper part, glycolysis will not activate in starved yeast presented with glucose

If a yeast cell would not have its overexpressed upper glycolytic enzymes when glycolysis is downregulated, a sudden increase in glucose will increase the efficiency of its enzymes, but the flux through upper glycolysis is then severely limited. In our model this is represented by low V_1. The higher the expression of upper glycolytic

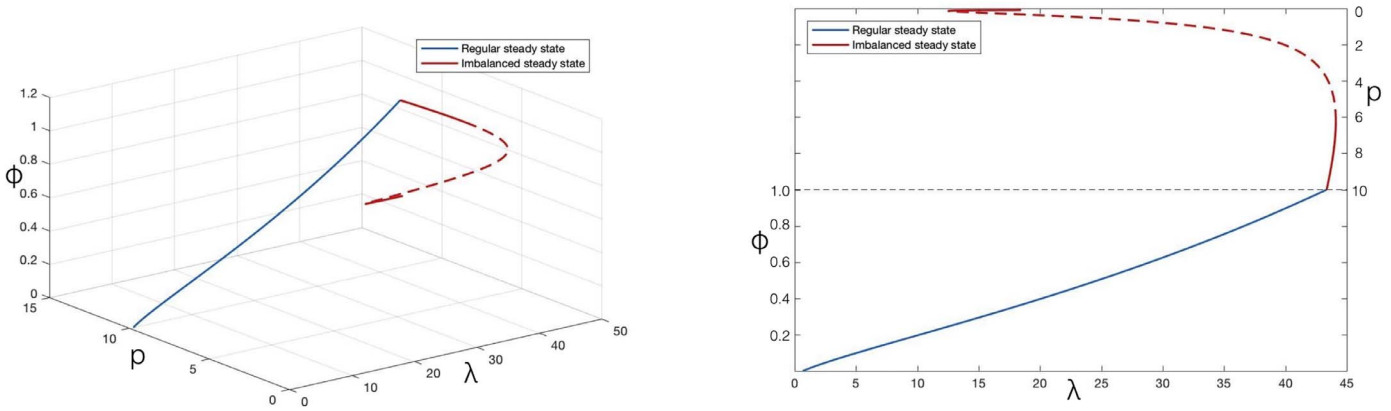

Fig. 8. The steady state curve for the transformed variable ϕ, reaching $\phi = 1$ (i.e., $f = \infty$, in blue) and the imbalanced states branching off from this (red). Left: bifurcation curves in (p, λ, ϕ)-space; Right: the same curves, showing the p and ϕ values along the curve, to better illustrate the bistability between regular and imbalanced states. See SI for parameter settings. (For interpretation of the references to colour in this figure legend, the reader is referred to the web version of this article.)

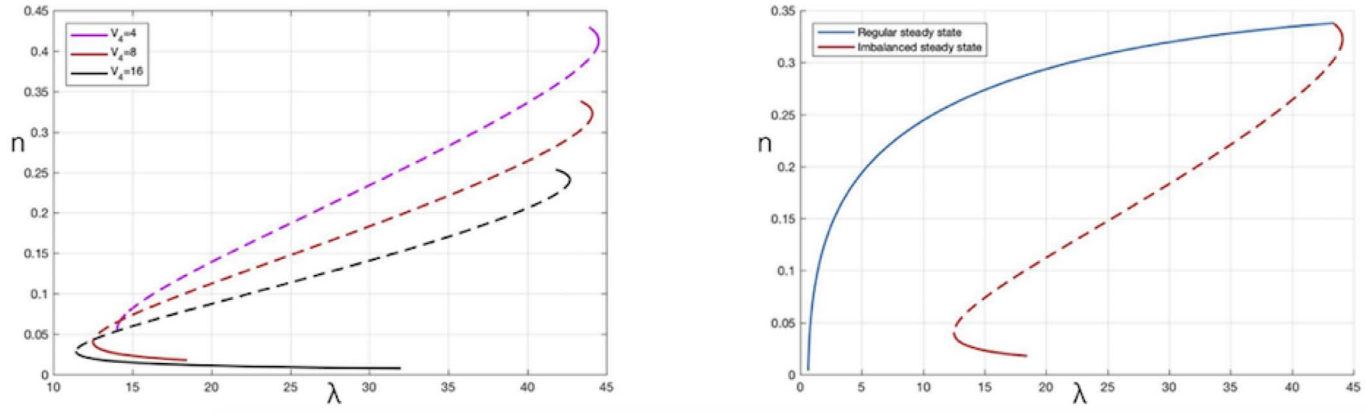

Fig. 9. The NADH concentration n as a function of λ. Left: for $V_4 = 4$, $V_4 = 8$, $V_4 = 16$ the imbalanced state curves are plotted in magenta, red and black respectively. Right: the regular steady states and imbalanced states for $V_4 = 8$. Parameter settings are discussed in the SI. (For interpretation of the references to colour in this figure legend, the reader is referred to the web version of this article.)

enzymes, the bigger V_1 may become when glucose is supplied.

Our analysis shows that there is a bifurcation from inactive to active glycolysis for $V_1 = V_6/2$ (Theorem 3). This means that the pathway is not activated by an increase in glucose if there is no overexpression of the upper glycolytic enzymes. Such a clear division in active flux through glycolysis vs. equilibrium has been found before in a small core model, including essentially only reactions ν_1, ν_2 and ν_6 [1,3]. Here we show in a more involved core model with two side-branches and ATP and NADH householding that this bifurcation value persists; the expression of the other enzymes in fermentative glycolysis do not influence the activation threshold.

4.2. Under mild conditions, FBP will function as a flux sensor on the metabolic scale

Theorem 4 shows that f increases along the family of regular steady states. This means it can act as a signal to the regulatory network and its value represents the current flux. Of course the regulatory network will then adjust transcription for the enzymes and the steady state flux and FBP concentration will be changed again, so there is some discrepancy to our analysis and the working of a flux sensor. However, on the metabolic scale it may act as a flux sensor.

4.3. Confirmation of bistable imbalanced state

The imbalanced state was not shown to exist with analysis, but through numerical continuation. We confirmed the existence of imbalanced states and rescue mechanisms. The steady state curve continues to infinite FBP, $\phi = 1$, of infinite pyruvate, $\rho = 1$, and it is possible to control the end point at infinity by changing V_4. From there, V_7 may be changed freely (as it does not appear in the finite steady state analysis). This suggests that bistability between regular and imbalanced states are commonplace, and does not depend much on specific kinetic parameters.

4.4. To both activate glycolysis and avoid the imbalanced state, heterogeneity is key

Yeast has a highly dynamic environment, so populations of yeast need to adjust quickly when nutrients are available. Our analysis shows that the expression of upper glycolysis is caught between two pressures. On the one hand, it needs enough expression to start up glycolysis, where more expression means higher steady state flux. On the other hand, if the expression is too high, the bistable imbalanced state appears which may cause an ATP-depleted death cycle. What is more, these thresholds are both dependent on the external glucose concentration. For the fitness of the population, it is therefore key that there is heterogeneity in the expression of upper glycolysis. No matter what the specific concentration is of suddenly available glucose, some cells in the population will immediately activate glycolysis optimally and avoid the imbalanced state.

4.5. A simple condition for the transcritical bifurcation

The bifurcation from Theorem 3 occurs when $2V_1 = V_6$. The ratio of 1: 2 is exactly the ratio between the reactions ν_1 and ν_6 in the Elementary Flux Mode which represents the normal glycolytic flux through the pathway (25). This does not even take into account the other EFM which does involve the side branches and should account for a part of the glucose uptake, specifically the part that does not produce any ATP. As soon as the rate of glucose uptake can support the ATP consumption downstream, the system has an emerging stable steady state with balanced metabolism. So although the condition $V_1 > V_6/2$ would seem to be a bare minimum for stability, it is all that is required.

The subtle point in our proof where we see why this bare minimum is enough is in the power series expansion (7). If we insert this expansion in the flux functions (2), we get exactly that those in the main branch of glycolysis are t^2, while the side branch reactions ν_3 and ν_5 are of order t^3. Hence, near the equilibrium, the flux directly through glycolysis is dominating the glucose consumption.

As mentioned in Section 4.1, this simple transition had been reported before in a small core model of essentially the ν_1, ν_2 and ν_6 reactions [1,3]. However, the bifurcation behaviour was found to be more complicated when adding glycerol production in the ν_3 and phosphate householding in the ν_7 reaction [13]. In this intermediate model, there was a richer set of solutions than found both in [1,3] and in the current model. The addition of NADH/NAD householding and pyruvate to the core model studied in [13] has again simplified the bifurcation structure, despite the added metabolic complexity. The key difference with [13] seems to be that in that intermediate model there could be steady state flux through the glycerol branch without lower glycolysis, while flux balance analysis of the new model shows that that is impossible (see eq. (25)). This follows from the redox balance relating ν_3 to ν_5, and ν_5 needs lower glycolysis ν_2 to be active. The redox balance therefore seems to tie together the pathways more, simplifying dynamics.

4.6. Scope of the techniques and general outlook

In this paper we have used three main techniques to study the bifurcation structure of the moderately detailed pathway with explicit kinetics: EFMs, the Implicit Function Theorem, and coordinate transformations. Here we briefly discuss the generality of our approach to other (and larger) pathways.

The use of EFMs to construct alternative steady state equations (Proposition 9 in the SI) is general. This method will be of use particularly for models with between four to about ten independent variables; with less, one can oversee the recombination of rows easily, and with more equations there will be a combinatorial explosion in the number of EFMs, and they do not provide additional insight. For higher numbers of independent variables, Extremal Pathways might be more suitable than EFMs, as there are less of those, but at some point also these will become cumbersome to use.

The Implicit Function Theorem is the basis of the transcritical bifurcation. Furthermore it was used especially to prove that the regular steady states formed a single curve. The technique uses smaller subdeterminants of the complete Jacobian matrix, and the linearity of $V_{\max}$ parameters in reaction functions to prove that at least one subdeterminant is always nonzero. This technique scales in principle to much larger networks, and it should eventually be possible to prove in full generality whether a detailed model such as the ones by Teusink et al. [15] or Hynne et al. [9] have the same property.

Finally, we used coordinate transformations to reformulate the steady state equations, for two reasons: to exploit the linearity of fluxes in those equations, and to compactify the dynamics and study imbalanced states “at infinity”. In our case the inverse transformation could be explicitly calculated, but this is not to be expected for larger networks (unless they involve several smaller individual transformations between metabolites and fluxes). Moreover, the amount of work necessary to prove that v_3 parameterises the steady states was considerable, and was strongly dependent on the explicit choices of reaction rate functions, their product structure and whether they happened to be increasing or decreasing in their respective variables. We do not expect that such calculations are possible in much larger networks. On the other hand, setting up the transformation itself was straightforward, and already allowed the study of both regular steady states and imbalanced states.

Acknowledgements

GO and RP gratefully acknowledge funding from NWO through the NDNS+ cluster, grant 613.009.012. GO would also like to thank Sander Hille for his guidance during early ventures into this research.

Supplementary material

Supplementary material associated with this article can be found, in the online version, at doi:10.1016/j.mbs.2018.03.007.

References

[1] G. Buzi, U. Topcu, J. Doyle, Analysis of autocatalytic networks in biology, Automatica 47 (2011) 1123–1130.
[2] A. Chambers, E.A. Packham, I.R. Graham, Control of glycolytic gene expression in the budding yeast (saccharomyces cerevisiae), Curr. Genet. (29) (1995) 1–9.
[3] F. Chandra, G. Buzi, J. Doyle, Glycolytic oscillations and limits on robust efficiency, Science, 333 (2011) 187–192.
[4] R. Díaz-Ruiz, N. Avéret, D. Araiza, B. Pinson, S. Uribe-Carvajal, A. Devin, M. Rigoulet, Mitochondrial oxidative phosphorylation is regulated by fructose 1,6-bisphosphate. a possible role in crabtree effect induction? J. Biochem. 283 (40) (2008) 26948–26955.
[5] J.M. Gancedo, The early steps of glucose signalling in yeast, FEMS Microbiol. Rev. 32 (4) (2008) 673–704.
[6] A. Goldbeter, R. Lefever, Dissipative structures for an allosteric model, Biophys. J. 12 (1972) 1302–1315.
[7] M.A. Hossain, J.M. Claggett, S.R. Edwards, A. Shi, S.L. Pennebaker, M.Y. Cheng, J. Hasty, T.L. Johnson, Posttranscriptional regulation of gcr1 expression and activity is crucial for metabolic adjustment in response to glucose availability, Mol. Cell 62 (3) (2016) 346–358.
[8] D.H.E.W. Huberts, B. Niebel, M. Heinemann, A flux-sensing mechanism could regulate the switch between respiration and fermentation, FEMS Yeast Res. 12 (2012) 118–128.
[9] F. Hynne, S. Danø, P. Sørensen, Full scale model of glycolysis in *saccharomyces cerevisiae*, Biophys. Chem. 94 (2001) 121–163.
[10] L. Keren, J. Hausser, M. Lotan-Pompan, I.V. Slutskin, H. Alisar, S. Kaminski, A. Weinberger, U. Alon, R. Milo, E. Segal, Massively parallel interrogation of the effects of gene expression fevels on fitness, Cell, 166 (5) (2016) 1282–1294.e18.
[11] K. Kochanowski, B. Volkmer, L. Gerosa, B.R.H. van Rijsewijk, A. Schmidt, M. Heinemann, Functioning of a metabolic flux sensor in *escherichia coli*, Proc. Nat. Acad. Sciences USA, 110 (3) (2013) 1130–1135.
[12] S.G. Krantz, H.R. Parks, The Implicit Function Theorem. History, Theory and Applications, Birkhäuser, 2003.
[13] R. Planqué, J. Hulshof, F. Bruggeman, B. Teusink, Understanding bistability in yeast glycolysis using general properties of metabolic pathways, Math. Biosci. 255 (2014) 33–42.
[14] R. Planqué, J. Hulshof, B. Teusink, J. Hendriks, F.J. Bruggeman, Maintaining Maximal Metabolic Rates Using Gene Expression Control, 2017. https://doi.org/10.1101/115428.
[15] B. Teusink, J. Passarge, C.A. Reijenga, E. Esgalhado, C.C. van der Weijden, M. Schepper, M.C. Walsh, B.M. Bakker, K. van Dam, H.V. Westerhoff, J.L. Snoep, Can yeast glycolysis be understood in terms of in vitro kinetics of constituent enzymes? Testing biochemistry, Eur. J. Biochem. 267 (2000) 5313–5329.
[16] B. Teusink, M.C. Walsh, K. van Dam, H.V. Westerhoff, The danger of metabolic pathways with turbo design, Trends Biochem. Sci. 23 (5) (1998) 162–169.
[17] H. Uemura, D.G. Fraenkel, Glucose metabolism in GCR mutants of saccharomyces cerevisiae, Biol. Lett. 181 (15) (1999) 4719–4723.
[18] J.H. van Heerden, M.T. Wortel, F.J. Bruggeman, J.J. Heijnen, Y.J.M. Bollen, R. Planqué, J. Hulshof, S.A. Wahl, B. Teusink, Lost in transition: uncontrolled startup of glycolysis results in subpopulations of non-growing cells, Science 343 (2014) 987.